Development of multi-phase-field crack model to express crack propagation in polycrystal

Kento Oshima[1], *Tomohiro Takaki[1], and Mayu Muramatsu[2]

[1]Mechanical and System Engineering, Kyoto Institute of Technology,
Matsugasaki, Sakyo, Kyoto 606-8585, Japan
[2]Functional and Structural Damage Verification Group,
Advanced Manufacturing Research Institute,
National Institute of Advanced Industrial Science and Technology,
1-1-1 Higashi, Tsukuba 305-8561, Japan

*Corresponding author: takaki@kit.ac.jp

Abstract

It is vitally important to ensure the safety of brittle materials. Therefore, it is essential to deeply understand the interaction of the material's microstructure and crack propagation. In this study, we constructed a multi-phase-field crack model which can express both, grain growth and crack propagation. To evaluate the basic characteristics of the developed model, we performed two-dimensional crack propagation simulations in a bicrystal when a crack enters a grain boundary by changing the ratio of the grain boundary energy to the crack surface energy and a threshold value of elastic strain energy for crack propagation. As a result, it is confirmed that the model can reasonably determine the crack path, depending on those conditions. Furthermore, by performing crack propagation simulations in a polycrystal, it is concluded that the model can properly express transgranular and intergranular cracks.

Keywords: Multi-phase-field method, Crack propagation, Polycrystal, Fracture mechanics

Introduction

Ferroelectric ceramics are widely used for ceramic condensers due to their superior properties in terms of dielectricity and insulation. In order to ensure the safety of brittle ferroelectric ceramics, it is important that microcrack propagation leading to fracture is evaluated accurately. However, the details of fracture have not yet been understood because fracture phenomena in microstructure are very complicated (Abdollahi and Arias, 2012). It is essential to deeply understand the interaction of the material's microstructure and crack propagation, because these two factors are closely interrelated (Guo, Chang and Chen, 2012). There are many studies on the fracture behavior of ferroelectric ceramics (Landis, 2003; Sheng and Landis, 2007; Zhu and Yang, 1999). However, since a fixed crack is assumed in most of these studies, investigations to understand the interaction of the material's microstructure and crack propagation are required as soon as possible.

The finite element method is the most famous numerical approach to evaluate crack propagation. However, it needs complex remeshing operations around the crack tip (Nagashima, Omoto and Tani, 2003; Kim, Wakayama and Kawahara, 1995). In addition, it is difficult to track the crack tip in complex microstructures. Recently, phase-field crack models have been developed (Henry, 2008; Song, Soh and Ni, 2007). Because the phase-field method does not need to track the crack tip position, it is thought that it can show its strength in crack propagation simulations in complex microstructures. However, such a phase-field crack model has not yet been proposed.

In this study, we develop a multi-phase-field crack model which can express crack propagation in those parts of the microstructure where grain growth takes place. To evaluate the validity of this model, we performed two-dimensional crack propagation simulations in a bi- and a polycrystal.

Multi-phase-field crack model

In the framework of the general multi-phase-field method applied to problems like grain growth, we construct a multi-phase-field crack model that can simulate crack propagation and grain growth simultaneously. Here, we use the multi-phase-field model proposed by Steinbach and Pezzolla (Steinbach and Pezzolla, 1999).

Phase-field variable

We use multiple phase-field variables ϕ_1, ϕ_2, …, ϕ_n. Here, n is the number of grains and cracks and the phase-field variable ϕ_i is defined as $\phi_i = 1$ inside of grain or crack i and $\phi_i = 0$ in all other grains or cracks. ϕ_i changes smoothly and rapidly at the grain boundary and crack surface regions. The phase-field variable ϕ_i must satisfy the condition $\sum_{i=1}^{n} \phi_i = 1$ at a grid point.

Free energy functional

The free energy functional can be described as

$$F = \int_V f dV = F = \int_V \left(f = f_{doub} + f_{grad} + f_{elast} \right) dV \,, \tag{1}$$

where the double well potential f_{doub} and the gradient energy density f_{grad} are expressed as

$$f_{doub} = \sum_{i=1}^{n} \sum_{j=i+1}^{n} \left(W_{ij} \phi_i \phi_j \right), \tag{2}$$

$$f_{grad} = \sum_{i=1}^{n} \sum_{j=i+1}^{n} \left(-\frac{a_{ij}^2}{2} \nabla \phi_i \cdot \nabla \phi_j \right), \tag{3}$$

with W_{ij} and a_{ij} being the energy barrier height and the gradient coefficient, respectively, in the grain boundary between grain i and j. f_{elast} is the elastic strain energy density.

Time evolution equation

Substituting Eq. (1) into the Allen-Cahn equation yields the time evolution equation of the phase-field variable ϕ_i:

$$\frac{\partial \phi_i}{\partial t} = -\frac{2}{n} \sum_{j=1}^{n} M_{ij}^{\phi} \left[\sum_{k=1}^{n} \left\{ \left(W_{ik} - W_{jk} \right) \phi_k + \frac{1}{2} \left(a_{ik}^2 - a_{jk}^2 \right) \nabla^2 \phi_k \right\} + \left(\frac{\partial f_{elast}}{\partial \phi_i} - \frac{\partial f_{elast}}{\partial \phi_j} \right) \right], \tag{4}$$

where M_{ij}^{ϕ} is the phase-field mobility. The derivative of the elastic strain energy density is expressed as

$$\frac{\partial f_{elast}}{\partial \phi_i} - \frac{\partial f_{elast}}{\partial \phi_j} = \mp \frac{8}{\pi} \sqrt{\phi_i \phi_j} \left(f_e - f_c \right), \tag{5}$$

with

$$f_e = \frac{1}{2} C_{ijkl} \varepsilon_{ij} \varepsilon_{kl} \,. \tag{6}$$

Here, C_{ijkl} is the elastic coefficient tensor of a material; ε_{ij} is the strain tensor; and f_c represents the threshold value of the elastic strain energy for crack propagation. The subscripts only in Eq. (6) indicate tensor components. Here, Eq. (5) only works at the crack surface between a crack and the surrounding material. The sign of the right side becomes negative when i represents a crack and it becomes positive when i indicates bulk material. As a result, by substituting Eq. (5) into Eq. (4), the following final time evolution equation for ϕ_i can be obtained:

$$\frac{\partial \phi_i}{\partial t} = -\frac{2}{n}\sum_{j=1}^{n} M_{ij}^{\phi}\left[\sum_{k=1}^{n}\left\{\left(W_{ik} - W_{jk}\right)\phi_k + \frac{1}{2}\left(a_{ik}^2 - a_{jk}^2\right)\nabla^2\phi_k\right\} \mp \frac{8}{\pi}\sqrt{\phi_i\phi_j}\left(f_e - f_c\right)\right]. \tag{7}$$

Here, the gradient coefficient a_{ij}, the energy barrier height W_{ij}, and the phase-field mobility M_{ij}^{ϕ} can be related to material parameters by the following equations:

$$a_{ij} = \frac{2}{\pi}\sqrt{2\delta\gamma_{ij}}, \quad W_{ij} = \frac{4\gamma_{ij}}{\delta} \quad \text{, and} \quad M_{ij}^{\phi} = \frac{\pi^2}{8\delta}M_{ij}, \tag{8}$$

where δ is the grain boundary or crack surface thickness (both are assumed to be identical), γ_{ij} is the grain boundary energy, and M_{ij} is the grain boundary mobility.

Simulations of crack propagation in a bicrystal

The basic characteristics of the multi-phase-field crack model derived in the previous section are investigated by performing crack propagation simulations in a bicrystal. Here, we evaluate the effects of the grain boundary energy and the threshold value of elastic strain energy on crack propagation into a grain boundary. The computational model and the boundary conditions used in the present simulations are shown in Fig. 1. Here, we set $\phi_1 = 1$ in the crack, $\phi_2 = 1$ in grain 1 and $\phi_3 = 1$ in grain 2. The displacements of the left and bottom sides of the model are constrained to the *x*- and *y*-directions, respectively. The lattice size is set to $\Delta x = \Delta y = 1$ μm, and an initial crack has a length of 1/3 of the width of the computational domain. The constant strain rate of $\dot{\varepsilon} = 1\times10^{-2}$ /s is applied to the top surface. For ϕ_i, we set the zero Neumann condition in all boundaries. Moreover, the following parameters are used: grain boundary thickness of $\delta = 4\Delta x$, surface energy of the crack of $\gamma = 1$ J/m^2, and crack mobility of $M = 1\times10^{-5}$ m^4/Js. In case of the conditions illustrated in Fig. 1, the gradient coefficient a_{ij}, energy barrier height W_{ij}, and phase-field mobility M_{ij}^{ϕ} in Eq. (8) are expressed as

$$a_{ij} = \begin{bmatrix} 0 & a & a \\ a & 0 & a_{gb} \\ a & a_{gb} & 0 \end{bmatrix}, \quad W_{ij} = \begin{bmatrix} 0 & W & W \\ W & 0 & W_{gb} \\ W & W_{gb} & 0 \end{bmatrix} \text{, and } M_{ij}^{\phi} = \begin{bmatrix} 0 & M^{\phi} & M^{\phi} \\ M^{\phi} & 0 & 0 \\ M^{\phi} & 0 & 0 \end{bmatrix}, \tag{9}$$

where *a* with and without subscript stands for the grain boundary and crack surface, respectively. In the present simulations, we assumed that the grain boundaries have zero mobility, though the present model can simulate the crack propagation in microstructure where the grains grow.

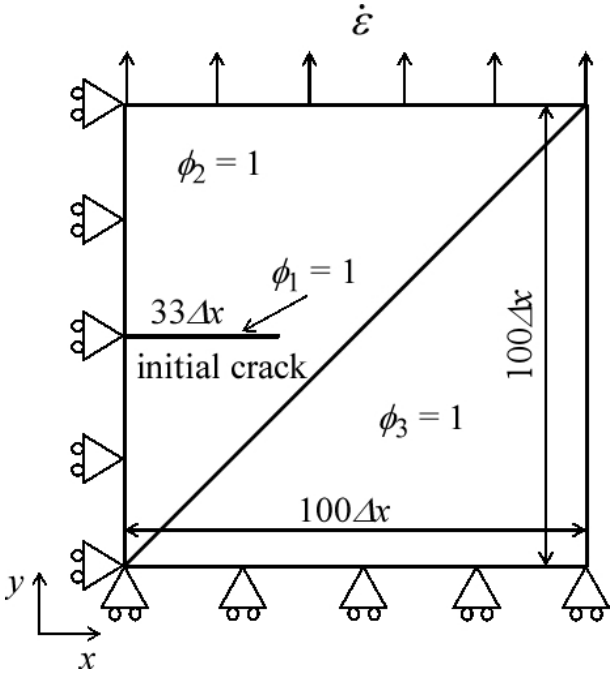

Figure 1. Computational model and boundary conditions for a bicrystal

Effect of grain boundary energy

The grain boundary energies γ_{gb} are set to 2.0γ, 1.7γ and 1.5γ. Figure 2 shows the calculated crack paths after crack propagation for three different grain boundary energies. In Fig. 2, the blue area represents the crack, the red areas represent grains 1 and 2 and the yellow line represents the grain boundary. As a result, we confirmed that the crack develops along the grain boundary for all grain boundary energies. In Fig. 2 (b) and (c), the crack propagates into grain 2 from the grain boundary. Because the crack path is determined in such a way as to reduce the total energy of the system, in case of small grain boundary energy, a larger energy benefit is obtained if the crack runs into the grain. We can also see that the crack progresses toward the lower left direction. The tendency is remarkable in case of larger grain boundary energy with larger tension. From the above, it is confirmed that the multi-phase-field crack model can represent the crack path in dependence of the grain boundary energy.

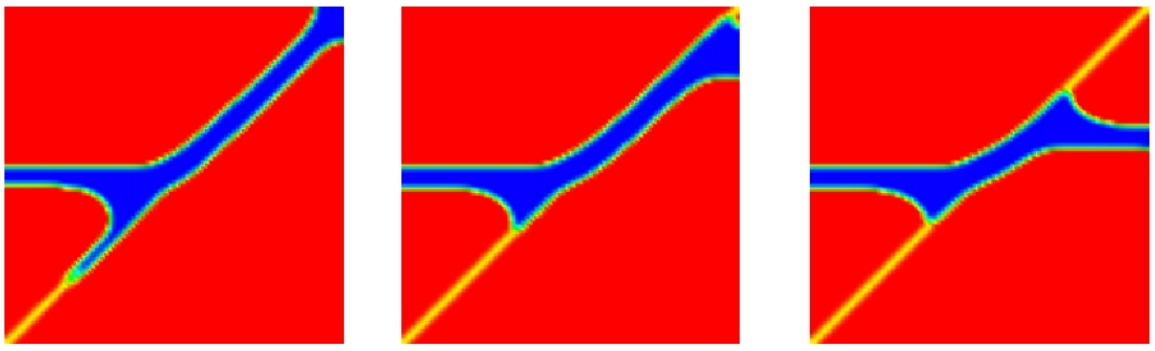

Figure 2. Crack propagation paths depending on the grain boundary energy

Effect of a threshold value of the elastic strain energy

The variable threshold values of the elastic strain energy used for crack propagation are 0.1 MPa, 0.5 MPa , and 1.0 MPa. Figure 3 shows the calculated crack path for three different threshold values. Here, we use $\gamma_{gb} = 2\gamma$. As evident from Fig. 3, it is observed that the crack propagation length in the grain boundary decreases with an increase of the threshold value. Moreover, the start time of crack propagation was delayed by increasing the threshold value. Therefore, it is confirmed that the threshold value of the elastic stain energy is appropriately incorporated into the model.

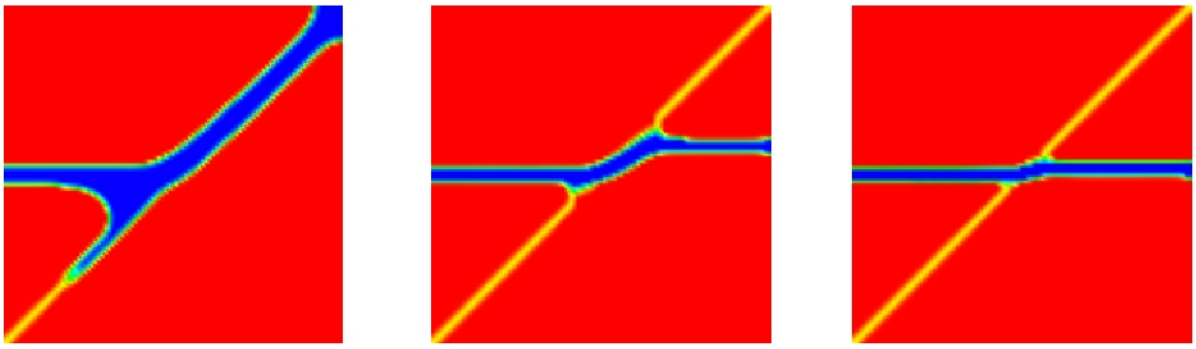

Figure 3. Crack propagation paths depending on the threshold value of the elastic strain energy

Simulation of crack propagation in a polycrystal

In this section, we perform a crack propagation simulation in a polycrystal by applying the multi-phase-field crack model. Figure 4 shows the time slices during crack propagation for a model size of $200\Delta x \times 100\Delta y$. In the numerical model, an initial crack of length $20\Delta x$ is placed at the center of the left side and 10 crystal grains are prepared. The other conditions are identical to those described in the previous section. Here, we use $\gamma_{gb} = 2\gamma$ and f_c = 0.5 MPa. From Fig. 4, we can see blue regions at some triple points in front of the crack tip. This phenomenon should not be considered strictly, because it is caused by the particular choice of the selected parameters. Nevertheless, it is observed that transgranular and intergranular cracks can be automatically represented in a polycrystal by the developed multi-phase-field crack model.

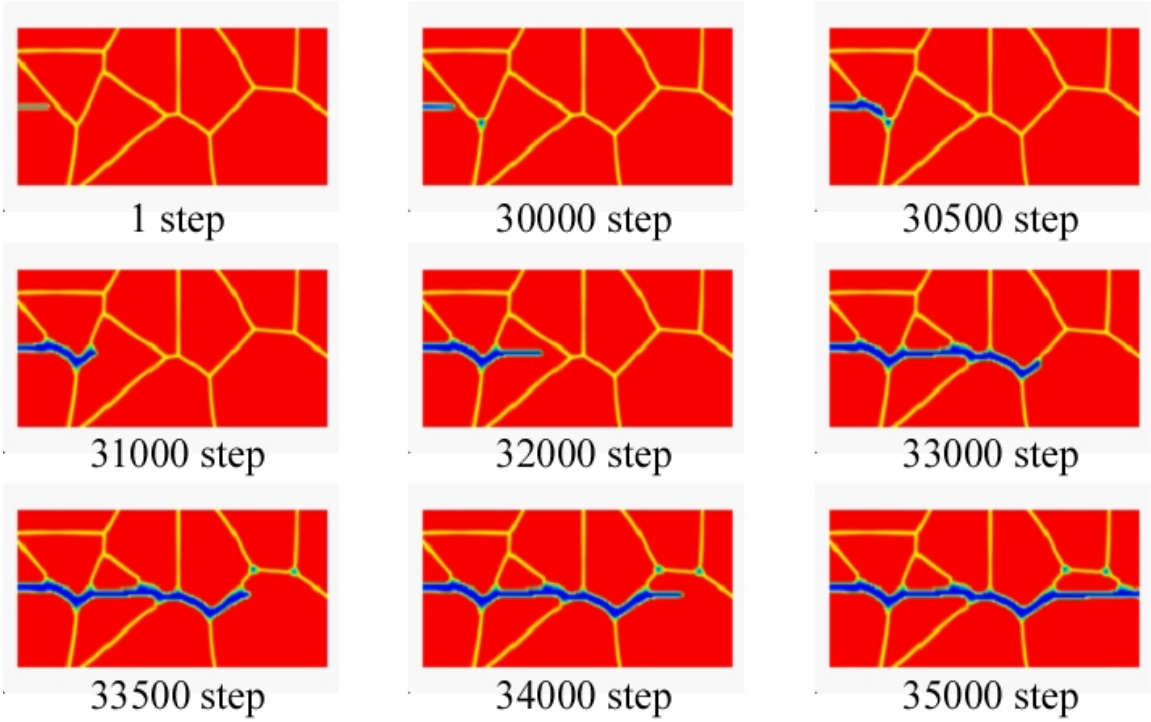

Figure 4. Time slices during crack propagation in a polycrystal

Conclusions

We developed a multi-phase-field crack model that can represent crack propagation and grain growth simultaneously. By performing two-dimensional crack propagation simulations in a bicrystal, the basic characteristics of the multi-phase-field crack model were evaluated by changing the ratio of the grain boundary energy to the surface energy of the crack surface and including a threshold value of the elastic strain energy. Furthermore, by performing crack propagation simulations in a polycrystal, it is concluded that the multi-phase-field crack model can appropriately represent transgranular and intergranular cracks.

References

Abdollahi, A. and Arias, I. (2012), Numerical simulation of intergranular and transgranular crack propagation in ferroelectric polycrystals. *International Journal of Fracture*. 174, pp.3-15.

Guo, X., Chang. K, and Chen, L. Q. (2012), Determination of fracture toughness of AZ31 Mg alloy using the cohesive finite element method. *Engineering Fracture Mechanics*. 96, pp.401-415.

Landis, C. M. (2003), On the fracture toughness of ferroelastic materials. *J Mech Phys Solids*. 51, pp.1347-1369.

Sheng, J. S. and Landis, C. M. (2007), Toughening due to domain switching in single crystal ferroelectric materials. *Int J Fract*. 143, pp.161-175.

Zhu, T. and Yang, W. (1999), Fatigue crack growth in ferroelectrics driven by cyclic loading. *J Mech Phys Solids*. 47, pp.81-97.

Nagashima, T., Omoto, Y. and Tani, S. (2003), Stress intensity factor analysis of interface cracks using X-FEM. *International Journal for Numerical Methods in Engineering*. 56, pp.1151-11773.

Kim, B., Wakayama, S. and Kawahara, M. (1995), Simulation of transgranular/intergranular crack propagation process in 2-dimensional polycrystals. *The Japan Society of Mechanical Engineers*. 61, pp.1241-1247.

Henry, H. (2008), Study of the branching instability using a phase field model of inplane crack propagation. *Europhysics Letters*. 83, pp.1-6.

Song, Y. C., Soh, A. K. and Ni, Y. (2007), Phase field simulation of crack tip domain switching in ferroelectrics. *J Phys D Appl Phys*. 40, pp. 1175-1182.

Steinbach, I. and Pezzolla, F. (1999), A generalized field method for multiphase transformations using interface fields. *Physica D*. 134, pp.385-393.